

Multifractal analysis of DNA walks and trails

Alexandre Rosas,¹ Edvaldo Nogueira, Jr.,^{1,2} and José F. Fontanari¹

¹*Instituto de Física de São Carlos, Universidade de São Paulo, Caixa Postal 369, 13560-970 São Carlos, SP, Brazil*

²*Instituto de Física, Universidade Federal da Bahia, Campus da Federação, 40210-340 Salvador, BA, Brazil*

(Received 16 September 2002; published 18 December 2002)

The characterization of the long-range order and fractal properties of DNA sequences has proved a difficult though rewarding task mainly due to the mosaic character of DNA consisting of many interwoven patches of various lengths with different nucleotide constitutions. We apply here a recently proposed generalization of the detrended fluctuation analysis method to show that the DNA walk construction, in which the DNA sequence is viewed as a time series, exhibits a monofractal structure regardless of the existence of local trends in the series. In addition, we point out that the monofractal structure of the DNA walks carries over to an apparently alternative graphical construction given by the projection of the DNA walk into the d spatial coordinates, termed DNA trails. In particular, we calculate the fractal dimension D_t of the DNA trails using a well-known result of fractal theory linking D_t to the Hurst exponent H of the corresponding DNA walk. Comparison with estimates obtained by the standard box-counting method allows the evaluation of both finite-length and local trends effects.

DOI: 10.1103/PhysRevE.66.061906

PACS number(s): 87.10.+e, 05.40.Fb, 47.53.+n

I. INTRODUCTION

The search for patterns in nature and their interpretation in terms of general principles is one of the main purposes of science. The explosive accumulation of DNA sequence data in the last two decades has provided a rich source of raw material that hides valuable hints about the evolutionary mechanisms of the genome organization. Unveiling the patterns in those sequences has become an exciting challenge to the present generation of statistical physicists and information scientists. In that vein, a truly remarkable result was the finding that intron-containing DNA coding regions exhibit long-range power-law correlations extending across more than 10^4 nucleotides, whereas intron-less coding regions display only short-range correlations [1,2].

Characterizing the long-range correlations in DNA sequences is a highly nontrivial task because of the mosaic structure of DNA consisting of patches with different nucleotide composition [3]. In fact, in order to use the standard techniques (e.g., power spectrum and R/S fluctuation analysis) to study the correlations of DNA sequences, it is necessary first to eliminate the local biases in nucleotide composition (trends), thus avoiding spurious effects due to the mosaic character of the sequence. In the context of time series or records, there are two main techniques to eliminate these trends, namely, the detrended fluctuation analysis (DFA) [2] and the wavelet transform (WT) [4]. The former is a physically appealing *ad hoc* technique of easy implementation and the latter is a mathematically well-established transform used to study the regularity of arbitrary functions via the systematic elimination of local polynomial behavior. Both techniques can be readily applied to the analysis of ordered linear sequences, such as DNA, by considering the reading direction as the time axis (see, e.g., Refs. [2,5] for the DFA and Refs. [6,7] for the WT analyses of DNA sequences).

A common strategy to represent graphically a given DNA sequence consists of transforming it into a d -dimensional random walk, so-called DNA walk, by associating a space

direction to each nucleotide (A, C, T, G) or class of nucleotides (e.g., purine and pyrimidine) and the time direction to the reading direction of the sequence [1]. Here, $A, C, T,$ and G are the bases adenine, cytosine, thymine, and guanine, respectively. In particular, a very popular representation is the one-dimensional walk, in which a purine (A or G) at position i is associated to one step down ($y_i = -1$) while a pyrimidine (T or C) is associated to one step up ($y_i = 1$). We note that the purine-pyrimidine classification is related to the hydrophobic-hydrophilic characteristics of the encoded amino acids. Of course, there are many alternative DNA walks and the most complete one that considers the four bases equivalently in base space is the three-dimensional DNA walk [8], in the sense that its projections on appropriate axes or planes recover all possible one- and two-dimensional walks.

For the sake of concreteness, in this section, we will focus on the fluctuations of the cumulative variable of the purine-pyrimidine random walk only, defined as

$$s(n) = \sum_{i=1}^n y_i \quad n = 1, \dots, N, \quad (1)$$

where N is the length of the sequence. This variable is displayed in Fig. 1 for the intron-rich human β -globin region (GenBank name HUMHBB), for which $N = 73\,326$ as well as for a shuffled sequence with same length and nucleotide composition. The statistical quantity that characterizes the fluctuations of $s(n)$ is the root mean square fluctuation $F_2(l)$ defined as

$$F_2(l) = \{[\overline{\Delta s(l)}]^2 - [\overline{\Delta s(l)}]^2\}^{1/2}, \quad (2)$$

where $\Delta s(l) = s(n+l) - s(n)$ and the bars indicate an average over all positions n in the record. We expect $F(l)$ to increase with increasing l , the length of the window considered. Explicitly, in the case of stationary series, the fluctuations are described by a power law

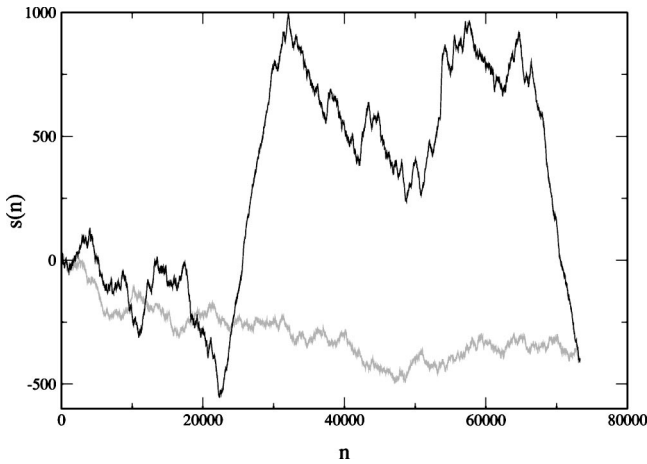


FIG. 1. Purine-pyrimidine random walk plot of the human β -globin region (black line) and a shuffled sequence of the same nucleotide composition (gray line).

$$F_2(l) \sim l^H, \quad (3)$$

where the scaling exponent (Hurst exponent) H equals $1/2$ in the case of random and short-ranged correlated sequences. Any value different from $1/2$ is the evidence of the existence of long-range correlations in the sequence [9–11]. In addition, for self-affine records (e.g., DNA walks), there is a simple relation between H and the local fractal dimension of the record, $D_r = 2 - H$. We note that the power-law behavior implies that there is no characteristic length scale, i.e., very large fluctuations are likely due to the same mechanisms as smaller ones.

Complex records are unlikely to be fully characterized by a single scaling exponent as evidenced by the case, where the scaling behavior is different in distinct parts of the series so that H is actually dependent on the part of the record being analyzed. A complete framework to describe the situation, where a multitude of scaling exponents is required is provided by the multifractal formalism [11,12] and, in this sense, the multifractal spectrum may be viewed as the ultimate tool to characterize a stationary time series. However, the direct calculation of $F_2(l)$ using Eq. (2) or the application of the standard multifractal formalism yields wrong results for nonstationary time series that are affected by local trends. In this contribution, we apply a generalization of the DFA recently proposed by Kantelhardt *et al.* for the characterization of nonstationary time series to study the multifractal properties of DNA walks [13]. In agreement with a previous multifractality analysis based on the wavelet transform modulus maxima (WTMM) method [6], we find that the DNA walks exhibit a simple monofractal scaling behavior. The multifractality analysis of one-dimensional DNA walks is the subject of Sec. II.

A seemingly alternative graphical representation of DNA sequences that has received less attention and so less criticism than the aforementioned DNA walks is the so-called DNA pseudo-random-walks [14–18]. They are simply the projection of the DNA walks into their d spatial components, i.e., the trails of the DNA walks. Of course, drawing these

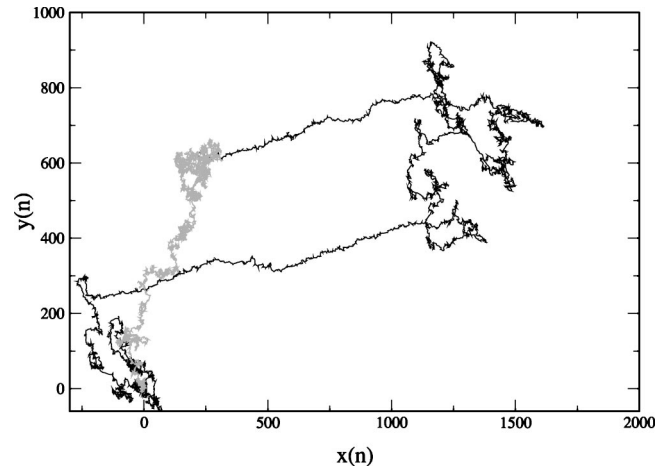


FIG. 2. Trail of the human β -globin region (black line) and a shuffled sequence of the same nucleotide composition (gray line) using the two-dimensional representation $T (x_i = 1)$, $A (x_i = -1)$, $G (y_i = 1)$, and $C (y_i = -1)$.

trails makes sense for $d \geq 2$ only, and Fig. 2 illustrates such a trail for a $d = 2$ representation of the HUMHBB sequence, where right, left, up, and down steps correspond to the presence of nucleotides T , A , G , and C , respectively. This representation preserves some basic symmetries of the DNA such as complementarity, reflection, substitution, and compatibility [15].

Despite the clear visual evidence of local trends in the trails exhibited in Fig. 2, it has been a common practice to apply standard fractal and multifractal methods (e.g., box counting [9] and sandbox [19]) to characterize their shapes without much concern about the mosaic structure of the underlying DNA sequence. Actually, the efforts focused on the understanding of the disturbing effects of the finite length of the sequences on the estimate of the fractal dimension D_t as well as on the multifractal characterization of the trail. For instance, although it is well known that in two dimensions, an infinite-length true random walk (i.e., a sequence of bases generated at random) is space filling and so $D_t = 2$, the box-counting and sandbox methods yield estimates significantly lower than 2 even for walks as large as 10^5 steps [15]. Moreover, finite-length random walks exhibit an effective multifractal spectrum mainly due to crossover effects between the usually distinct bulk and surface properties of the trail [16]. These caveats, however, have not prevented claims that relatively short (typically 2×10^4 bp) mitochondrial DNA genomes have a definite multifractal structure [18]. In Sec. III of this contribution, we invoke a classical result of fractal theory to link the Hurst exponent of the DNA walk to the fractal dimension of the corresponding trail in space (see, e.g., Refs. [9,10]) then arguing in favor of the monofractality of DNA trails too.

II. DNA WALKS

Consider a record, such as that given in Eq. (1), where the variables y_i are not necessarily Ising variables but must form a compact support, i.e., $y_i = 0$ for a very small fraction of the

elements only. The generalized multifractal DFA (MF-DFA) involves the following steps (we refer the reader to Ref. [13] for a thorough presentation of the method). First, divide the entire sequence into $N_l = \text{int}(N/l)$ nonoverlapping segments of length l . Second, for each segment $\nu = 1, \dots, N_l$ of length l , calculate the local trend by a least-square fit of the record in the segment, and denote by $s_\nu(n)$ the fitting polynomial in segment ν . Then evaluate the variance

$$F^2(l, \nu) = \frac{1}{l} \sum_{n=1}^l \{s[(\nu-1)l+n] - s_\nu(n)\}^2 \quad (4)$$

for each segment. An important parameter is the order $m = 0, 1, 2, \dots$ of the polynomial $s_\nu(n)$ used in the fitting procedure. The choices of m correspond to different orders of DFA, denoted by DFA m , which differ in their capability of eliminating trends in the series. For instance, DFA0 can eliminate only constant trends in the series, DFA1 eliminates constant as well as linear trends, and so on, so that a comparison of the results for different orders of DFA yields information on the type of trend in the series. Third, determine the order q fluctuation function averaging over all segments,

$$F_q(l) = \left\{ \frac{1}{N_l} \sum_{\nu=1}^{N_l} [F^2(l, \nu)]^{q/2} \right\}^{1/q}, \quad (5)$$

where, in general, the index variable q takes on any real value, except zero. As the final step, analyze log-log plots of $F_q(l)$ versus l for each value of q in order to determine the scaling behavior of the fluctuation functions. For large values of l , we expect these functions to increase with increasing l as a power law

$$F_q(l) \sim l^{h(q)}. \quad (6)$$

Clearly, for $q=2$, one has $h(2)=H$ by construction, and in the case that the scaling behavior of $F^2(l, \nu)$ is identical for all segments ν , i.e., the record is a monofractal, the exponent $h(q)$ is independent of q as expected. The definition (5) is well suited to detect discrepancies in the scaling behavior of the large and small fluctuations. In particular, for positive q , $h(q)$ yields the scaling behavior of the segments with large fluctuations while for negative q , $h(q)$ yields the scaling of the segments with small variances. In addition, there is a simple relation between $h(q)$ and the scaling exponents $\tau(q)$ defined by the standard partition function-based multifractal formalism [13],

$$\tau(q) = qh(q) - 1. \quad (7)$$

The importance of this relation is that it allows comparison of the results obtained in the MF-DFA scheme with those of the standard multifractal analysis in the case of stationary series, and with those of the WTMM in the case of nonstationary series.

In Fig. 3, we show the multifractal spectrum $\tau(q)$ obtained by the application of different orders of the MF-DFA method to the intron-rich HUMHBB sequence. The results for orders larger than five are indistinguishable in the scale of

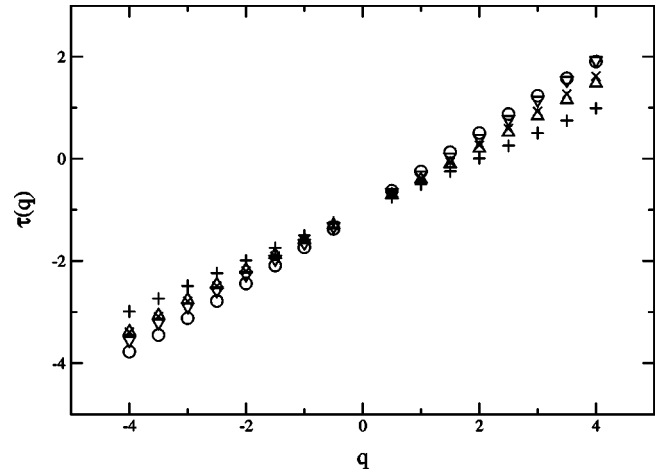


FIG. 3. Multifractal spectrum $\tau(q)$ vs q for the DNA walk of the intron-rich HUMHBB sequence depicted in Fig. 1. The data correspond to different orders of DFA, $m=0$ (\circ), 1 (∇), 3 (\times), and 5 (\triangle). The symbol + corresponds to the data for the shuffled sequence.

the figure, so the data for $m=5$ (\triangle) yields the trendless spectrum. Analysis of this figure gives valuable information on the nature of the correlations of the DNA walk. In particular, the linearity of the trendless spectrum indicates that the record $s(n)$ depicted in Fig. 1 is monofractal. Actually, this conclusion is not affected by the presence of trends in the series, since the q dependence of $\tau(q)$ is linear regardless of the value of m . However, the value of the scaling exponent $H = h(q) \forall q$, given by the slope of the straight lines that fit the data, is sensitive to local trends. For example, we find $H = 0.72 \pm 0.02$ for $m=0$, $H = 0.68 \pm 0.02$ for $m=1$, and $H = 0.60 \pm 0.02$ for $m=5$. As expected, $H = 0.50 \pm 0.02$ for the shuffled sequence. All these numerical values are in perfect agreement with the values obtained using the WTMM method [6]. Since the trendless scaling exponent is definitively different from $1/2$, we can conclude for the existence of long-range correlations in this particular intron-containing sequence. The long-range correlation induced by the local trends is reflected in the larger value of the scaling exponent calculated with the MF-DFA0, which overestimates the value of H in about 20%. It is interesting to note that the trends influencing the large fluctuations ($q > 0$) are practically unaffected by the application of DFA1.

The results of the application of the MF-DFA method to the characterization of a sequence composed predominantly of coding regions is summarized in Fig. 4. The sequence considered is a portion of the *E. coli* K12 genome (GenBank name ECO110K), for which $N = 111\,401$. We find $H = 0.60 \pm 0.02$ for $m=0$ and $H = 0.51 \pm 0.02$ for $m \geq 1$ as well as for the shuffled sequence. As before, the monofractal structure of the record is confirmed by the linearity of the $\tau(q)$ spectrum. Moreover, failure to eliminate the local trends leads to a wrong conclusion about the existence of long-range correlations in this DNA walk, as evidenced by the overestimate of H that results from the application of MF-DFA0. The local trends in this sequence seem to have a particularly simple linear nature since application of MF-DFA1 is sufficient to eliminate them altogether.

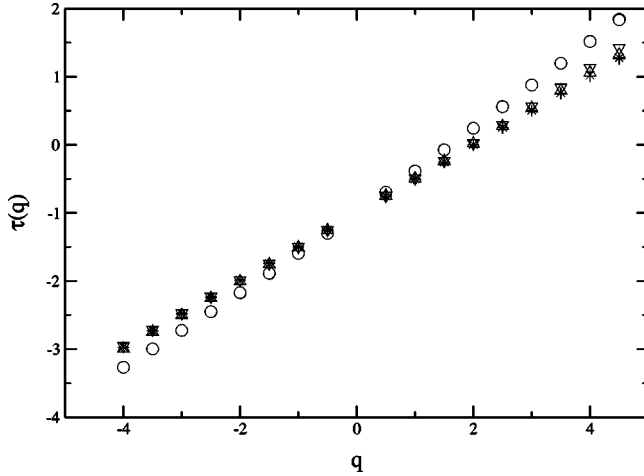


FIG. 4. Same as Fig. 3 but for the DNA walk of the *E. coli* chromosomal sequence ECO110K composed primarily of coding regions.

To conclude this section, we note that we have considered several alternative one-dimensional representations, such as the strong-weak bond classification, where *C* or *G* are associated to one step up ($y_i=1$) and *A* or *T* to one step down ($y_i=-1$). All the alternative schemes analyzed have produced within the numerical precision exactly the same exponents of the purine-pyrimidine classification. Our results could also be obtained within the WTMM framework and, in fact, the wavelet analysis of the HUMHBB sequence can be found in Ref. [6]. The aim of this section was to give additional support to the claim of Kantelhardt *et al.* that, despite the operational and conceptual simplicity of the MF-DFA method, it yields results that are identical to those derived by the sophisticated WTMM method [13]. For instance, this easiness of implementation has allowed us to study higher-dimensional DNA walks, an awkward task to be carried out using the WTMM method, for several representations proposed in the literature (see, e.g. Refs. [8,15,17,18]). As we will show in the sequel, the results were essentially the same as those reported here for the one-dimensional DNA walks.

III. DNA TRAILS

As pointed out before, a DNA trail is the projection of a two-dimensional DNA walk into the space plane. Figure 5 shows the time record of the walk that gives rise to the trail illustrated in Fig. 2 for the HUMHBB sequence. We begin by noting that the generalization of the MF-DFA method to two- or higher-dimensional records is straightforward as one needs only to change the basic Eq. (4), which is rewritten as

$$\hat{F}^2(l, \nu) = \frac{1}{l} \sum_{n=1}^l \{s[(\nu-1)l+n] - s_\nu(n)\}^2, \quad (8)$$

where $s(n) = x(n)\mathbf{i} + y(n)\mathbf{j}$ and similarly for the fitting polynomial vector s_ν . Over an interval of l steps, the position vector in the trail will vary by typically $|\delta\mathbf{r}| \approx F_2(l) = l^H$ while the “mass” M of the trail, i.e., the number of points generated by these steps is $M \sim l$, provided the contribution

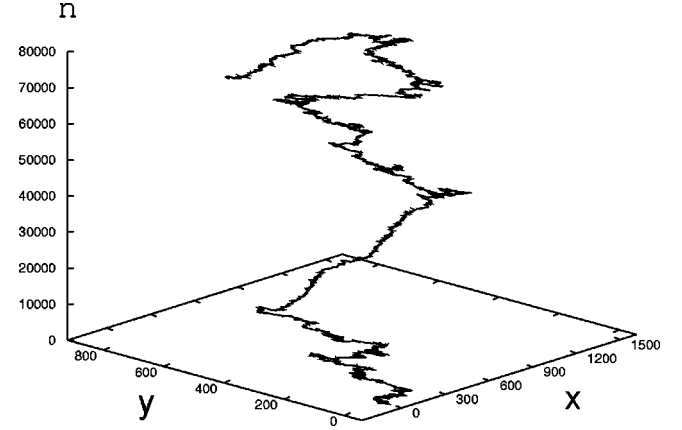


FIG. 5. Two-dimensional DNA-walk representation of the HUMHBB sequence whose projection into the space plane yields the trail of Fig. 2.

of overlapping points is negligible. Hence $M \sim |\delta\mathbf{r}|^{1/H}$, from where one concludes that $D_t = 1/H$. This relation is valid only if $1/H < d$, where d is the space dimension. When $1/H > d$, overlap cannot be neglected and so $D_t = d$ (see Refs. [9,10] for mathematical and pictorial details of this argument). Thus, knowledge of the Hurst exponent H for the d -dimensional DNA walks determines uniquely the fractal dimension of the DNA trail. Calculation of H or, more generally, of $h(q)$ follows the same procedure sketched before for the one-dimensional case, except that the variance given in Eq. (4) is now replaced by \hat{F}^2 .

Application of the MF-DFA method to two-dimensional DNA walks representing the HUMHBB (see Fig. 5) and the ECO110K sequences yields, within the numerical precision, the same results as for the one-dimensional case. Actually, so far as the value of the Hurst exponent H is concerned, this agreement is expected since using Eqs. (8) and (5) for $q=2$, we have simply $F_2 \sim l^{H_x} + l^{H_y}$, where H_x and H_y are the scaling exponents of the one-dimensional DNA walks in the plane (n, x) and (n, y) . Hence for large l , one has $H = \max(H_x, H_y)$. In Table I, we present the estimate of the fractal dimension D_t of the HUMHBB and ECO110K trails, as well as of a random trail characterized by the same length and base frequency as the ECO110K sequence. The errors in the estimates of D_t are statistical errors. For the box-counting method, the systematic errors are probably much larger than those shown in Table I, due mainly to finite-length effects [16].

TABLE I. Estimates of the fractal dimension D_t of two-dimensional trails. The MF-DFA estimates are based on the formula $D_t = 1/H$, where H is the Hurst exponent of the record (e.g., Fig. 5). The box-counting method is applied directly to the trail (e.g., Fig. 2).

Sequence	N	MF-DFA5	MF-DFA0	Box counting
HUMHBB	73 326	1.67 ± 0.06	1.39 ± 0.04	1.40 ± 0.01
ECO110K	111 401	1.96 ± 0.08	1.67 ± 0.06	1.38 ± 0.01
Random	111 401	2.00 ± 0.08	2.00 ± 0.08	1.45 ± 0.01

Interestingly, although the D_t estimates of the MF-DFA method are based on the analysis of finite-length records, this has practically no effect on the results, as evidenced by the correct calculation of D_t for the random sequence, a test which the box-counting method clearly fails. Moreover, these data corroborate the intuition, stemming from the visual inspection of Fig. 2, that the effect of the local trends is to decrease the fractal dimension of the trail. The excellent agreement between the box-counting estimate, which is affected by both local trends and finite-length effects, and the MF-DFA0 estimate, which is affected by local trends only, indicates that the surface effect is negligible for the HUMHBB sequence. In fact, this is expected since the box-counting method is very reliable to calculate the fractal dimensions of structures that do indeed exhibit fractality, predictably failing in the case of space-filling structures. The results for the ECO110K sequence illustrate the bad performance of box counting when the two sources of systematic errors are present. The aforementioned agreement between the box-counting and the MF-DFA0 methods demonstrates unequivocally that the spurious effects of local trends must be filtered out for a correct account of the fractal or multifractal properties of DNA trails, a procedure that has been ignored in all previous analyses presented in the literature [8,14–18].

Since the MF-DFA analysis has indicated that even the higher-dimensional DNA walks are monofractals, one concludes that the variance $\hat{F}^2(l, \nu)$ defined in Eq. (8) is the same for all segments ν of the record. As a result, the variation of the position vector $|\delta\mathbf{r}|$ in the trail will be independent of the segment ν and so the trail must have a monofractal structure too. This conclusion seems at odds with those of multifractal analyses based on the sandbox and box-counting methods [16–18]. However, we note that the original claim of Ref. [16] was that finite-length DNA trails, as well as randomly generated trails, are characterized by *effective* multifractal spectra. Clearly, these spectra are artifacts of the sandbox and box-counting methods, which cannot deal adequately with the surface effects. The unjustified dropping of the adjective “effective” [17,18] led then to the apparent disagreement between the two approaches. These effective multifractal spectra might indeed be an useful tool for comparing random or biological sequences of similar lengths [17], especially if one manages to free them from the local trends effects.

IV. CONCLUSION

The main purpose of this contribution was to point out that the statistical properties of two apparently distinct and pictorially appealing representations of DNA sequences, namely, DNA walks (Figs. 1 and 5) and DNA trails (Fig. 2) are in fact closely related. In particular, we argued that the

patchiness of the DNA sequences, which has greatly hindered the characterization of the long-range correlations of DNA walks [2,3] also plagues the fractal and multifractal analyses of the DNA trails, a fact that has been largely overlooked in previous investigations [16–18]. Using the recently proposed multifractal detrended fluctuation analysis (MF-DFA) method [13] to filter the local trends of DNA walks in $d=1$ and 2 dimensions, we were able to show that these walks are monofractals. This conclusion holds true for the nondetrended walks as well, since the multifractal spectrum $\tau(q)$ is linear regardless of the order $m \geq 0$ of the fitting polynomials used to eliminate the local trends (Figs. 3 and 4). More importantly, the independence of the variance $F^2(l, \nu)$ [see Eqs. (4) and (8)] on the segment ν of the DNA walk carries over to the DNA trail, which is thus monofractal too. In particular, the fractal dimension of the trail is $D_t = 1/H$, where H is the Hurst exponent of the record [9,10]. In the case $1/H > d$, as for the one-dimensional walks, one has $D_t = d$. Although we have presented data for the HUMHBB and the ECO110K sequences only, which probably are, respectively, the most popular examples of intron-rich and intron-poor sequences, we have verified that our main results hold true for many other sequences in the GenBank.

Once one has discarded the simple local variations in nucleotide composition along DNA sequences as the cause of the long-range correlations observed in intron-rich sequences (though these variations *do* cause the spurious long-range correlations in intron-poor sequences), it is natural to ask then what are the sources for these correlations, which, as shown above, are also responsible for the nontrivial (fractal) geometry of the DNA trails. The answer is that neither the internal structure of patches nor their order in the sequence are relevant: it is the power-law distribution of patch lengths that determines the true long-range correlations [5]. This as well as several other findings concerning the statistical properties of DNA sequences have prompted the proposal of minimal evolutionary models, based on biologically motivated mechanisms, to account for those features (see, e.g., Refs. [20–22]). In fact, rather than providing measures to characterize or distinguish classes of sequences, we think that the thrust of the research on large-scale statistical properties of genomes is to provide quantitative standards for modeling the inherently stochastic process of molecular evolution [23], bearing thus on fundamental issues such as the origin of life and the evolution of complexity [24].

ACKNOWLEDGMENTS

This research was supported by Fundação de Amparo à Pesquisa do Estado de São Paulo (FAPESP), Project No. 99/09644-9. The work of J.F.F. was supported in part by Conselho Nacional de Desenvolvimento Científico e Tecnológico (CNPq).

[1] C.-K. Peng, S.V. Buldyrev, A.L. Goldberger, S. Havlin, F. Sciortino, M. Simons, and H.E. Stanley, *Nature (London)* **356**, 168 (1992).

[2] C.-K. Peng, S.V. Buldyrev, S. Havlin, M. Simons, H.E. Stanley, and A.L. Goldberger, *Phys. Rev. E* **49**, 1685 (1994).

[3] S. Karlin and V. Brendel, *Science* **259**, 677 (1993).

- [4] C. K. Chui, *An Introduction to Wavelets* (Academic Press, Boston, 1992).
- [5] P. Bernaola-Galván, R. Román-Roldán, and J.L. Oliver, Phys. Rev. E **53**, 5181 (1996).
- [6] A. Arneodo, E. Bacry, P.V. Graves, and J.F. Muzy, Phys. Rev. Lett. **74**, 3293 (1995).
- [7] A.A. Tsonis, P. Kumar, J.B. Elsner, and P.A. Tsonis, Phys. Rev. E **53**, 1828 (1996).
- [8] L. Luo, W. Lee, L. Jia, F. Ji, and L. Tsai, Phys. Rev. E **58**, 861 (1998).
- [9] B. B. Mandelbrot, *The Fractal Geometry of Nature* (Freeman, San Francisco, 1982).
- [10] R.F. Voss, Physica D **38**, 362 (1989).
- [11] J. Feder, *Fractals* (Plenum Press, New York, 1988).
- [12] T.C. Halsey, M.H. Jensen, L.P. Kadanoff, I. Procaccia, and B.I. Shraiman, Phys. Rev. A **33**, 1141 (1986).
- [13] J.W. Kantelhardt, S.A. Zschiegner, E. Koscielny-Bunde, A. Bunde, S. Havlin, and H.E. Stanley, e-print physics/0202070.
- [14] M.A. Gates, J. Theor. Biol. **119**, 319 (1986).
- [15] C.L. Berthelsen, J.A. Glazier, and M.H. Skolnick, Phys. Rev. A **45**, 8902 (1992).
- [16] C.L. Berthelsen, J.A. Glazier, and S. Raghavachari, Phys. Rev. E **49**, 1860 (1994).
- [17] J.A. Glazier, S. Raghavachari, C.L. Berthelsen, and M.H. Skolnick, Phys. Rev. E **51**, 2665 (1995).
- [18] N.N. Oiwa and J.A. Glazier, Physica A **311**, 221 (2002).
- [19] T. Vicsek, *Fractal Growth Phenomena* (World Scientific, Singapore, 1992).
- [20] W. Li, Phys. Rev. A **43**, 5240 (1991).
- [21] P.M.C. de Oliveira, Physica A **273**, 70 (1999).
- [22] Y. Almirantis and A. Provata, BioEssays **23**, 647 (2001).
- [23] M. Kimura, Theor Popul. Biol. **2**, 174 (1971).
- [24] J. T. Bonner, *The Evolution of Complexity* (Princeton University Press, Princeton, 1988).